ACS Macro Letters

Letter

pubs.acs.org/macroletters

Fast Nanorod Diffusion through Entangled Polymer Melts

Jihoon Choi,[†] Matteo Cargnello,[‡] Christopher B. Murray,[‡,§] Nigel Clarke,[∥] Karen I. Winey,[§] and Russell J. Composto*[,§]

[†]Department of Materials Science and Engineering, Chungnam National University Daejeon, South Korea

Departments of [‡]Chemistry and [§]Materials Science and Engineering, University of Pennsylvania, Philadelphia, Pennsylvania, United States

[∥]Department of Physics and Astronomy, University of Sheffield, Sheffield, United Kingdom

Supporting Information

ABSTRACT: Nanorod diffusion in polymer melts is faster than predicted by the continuum model (CM). Rutherford backscattering spectrometry is used to measure the concentration profile of titanium dioxide (TiO_2) nanorods (L = 43 nm, d = 5 nm) in a polystyrene (PS) matrix having molecular weights (M) from 9 to 2000 kDa. In the entangled regime, the tracer diffusion coefficients (D) of TiO_2 decrease as the $M^{-1.4}$, whereas the CM predicts $D_{CM} \sim M^{-3.0}$ using the measured zero-shear viscosity of TiO_2(1 vol %): PS(M) blends. By plotting D/D_{CM} versus M/M_e, where M_e is the entanglement molecular weight, diffusion is enhanced by a factor of $10-10^3$ as M/M_e increases. The faster diffusion is attributed to decoupling of nanorod diffusion from polymer relaxations in the surrounding matrix, which is facilitated by the nanorod dimensions (i.e., L greater than and d less than the entanglement mesh size, 8 nm).

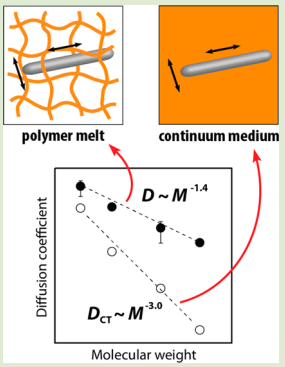

Nanoparticle (NP) diffusion plays a key role in the design and function of polymer nanocomposites, because NP mobility impacts whether NPs disperse or aggregate due to favorable or unfavorable mixing, respectively, in homopolymer matrices.[1−3] In multiphase nanocomposites containing NPs and block copolymer, the partitioning of NPs within a specific domain requires rapid mobility of NPs relative to the slower polymer rearrangement during assembly.[4] Thus, an understanding of NP diffusion is important for designing and fabricating new hybrid materials for microelectronics, light management, and energy applications,[5−7] which rely on precise control over the lateral and vertical positioning of NPs in polymer films.

Traditionally, diffusion of large spherical NPs in a continuous medium has been described by the Stoke−Einstein (SE) relation $D_{SE} = (1/f\pi)\ (k_BT/\eta R)$, where k_B is the Boltzmann constant, T is absolute temperature, η is the pure solvent viscosity, and R is the NP radius. The constant f is 4 or 6, depending on whether there is slip or nonslip conditions at the particle/medium interface, respectively. However, for NPs smaller than the characteristic length scales of the medium, namely, the polymer radius of gyration (R_g) for unentangled polymer melt, correlation length (ξ) for a polymer solution, and tube diameter (d_t) for an entangled polymer melt, the SE relationship underestimates NP diffusion.[8−12] Note that the tube diameter is comparable to the entanglement mesh size in an entangled polymer melt. As pointed out by Brochard Wyart and de Gennes,[13] for such conditions, the continuum fluid assumption fails, because flow around small particles is no longer captured by the viscosity η. Rather, depending on NP size relative to the characteristic lengths (R_g and d_t for melts), the local friction experienced by the NP is reduced if the particle diameter is less than the Navier extrapolation length (order of microns). A recent study investigated the effect of NP size on diffusion in polymer melts and found that D/D_{SE} increased as $2R/d_t$ decreased.[11]

In the limit of small ($2R/d_t \ll 1$) and large ($2R/d_t \gg 1$) NP sizes, NP motion in a polymer melt is well understood by theory or molecular dynamics (MD) simulations.[13,14] Based on the size of NPs relative to the polymer chains, the motion of large NPs in a highly entangled polymer melt is strongly constrained by chain entanglements that relax via reptation (i.e., $D \sim \eta^{-1} \sim M^{-3.4}$), whereas chain disentanglement is not required for very small NPs because the entanglement mesh contains free space for monomeric units to rearrange and accommodate NP motion.[13] Recent MD simulations by Kalathi et al. provide a more detailed understanding of NP dynamics as a function of matrix molecular weight and NP size.[14] Although a majority of studies involve spherical NPs, the diffusion of anisotropic NPs is important for understanding the processing of nanocomposite devices[15] and transport in crowded biological materials.[16]

Nanorod (NR) motion is described by hydrodynamic theory that relates the translational diffusion coefficient, D_{CM}, to the friction coefficient ξ by the Einstein relation $D = k_BT/\xi$. In

Received: May 25, 2015
Accepted: August 17, 2015
Published: August 20, 2015

DOI: 10.1021/acsmacrolett.5b00348
ACS Macro Lett. 2015, 4, 952−956

terms of parallel and perpendicular diffusion along the NR axis in a continuous medium (Figure 1a), D_{CM} is

$$D_{CM} = (D_{||} + 2D_{\perp})/3 \quad (1)$$

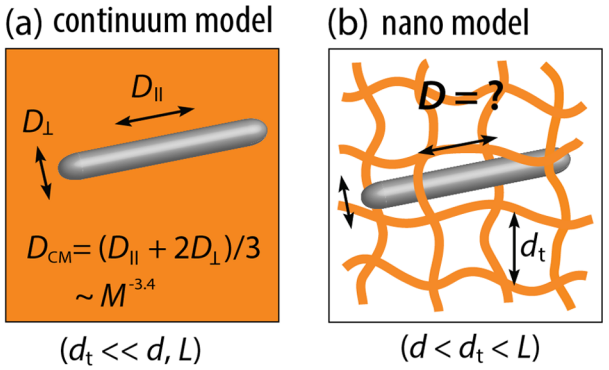

Figure 1. (a) Schematic of a nanorod (NR) of diameter d and length L in a matrix having an entanglement mesh size (d_t) much smaller than d and L. This continuous medium model results in the Einstein relation where diffusion scales inversely with the matrix viscosity. (b) When the entanglement mesh size is greater than d but less than L, NR diffusion is faster due to reduced local friction for parallel NR diffusion.

Here, parallel and perpendicular diffusion coefficients are

$$D_{||} = \frac{k_B T}{2\pi\eta L} \ln(L/d) \quad (2)$$

$$D_{\perp} = \frac{k_B T}{4\pi\eta L} \ln(L/d) \quad (3)$$

where d and L are NR diameter and length, respectively.[17] Eq 1 is in good agreement with experimental results for cylindrical particles moving in a continuum fluid, when ligand dimensions and boundary conditions are considered.[18−20] However, similar to spherical NPs, NRs are expected to show faster diffusion in a highly entangled polymer melt when the NR size becomes smaller than d_t ($d < d_t$). Recent study showed a deviation from continuum hydrodynamics for gold NRs diffusion in polyethylene glycol using a multiphoton fluctuation correlation spectroscopy technique.[21] For ultrathin NRs (i.e., $d < d_t$), Brochard-Wyart and de Gennes predicted that $D_{||}$ is determined by the local segmental friction, namely, $\eta_m(L/a)$, where η_m and a are the monomer viscosity and size, respectively.[13] However, $D_{\perp}$ is described by the friction due to the bulk viscosity (η_B) of the entangled polymer melt. Figure 1b shows NR diffusion perpendicular and parallel to the network formed by entangled matrix chains. Although theoretical predictions of anisotropic NP transport in a polymer melt have been proposed,[13] experimental studies that identify and understand important materials parameters are lacking.

In this letter, we measure the diffusion coefficients of nanorods (L = 43.1 nm, d = 4.6 nm) as a function of matrix molecular weight, which ranges from unentangled (M = 9 kDa) to highly entangled (2000 kDa), to test the validity of hydrodynamic theory and investigate the underlying polymer dynamics for conditions, where the nanorod diameter is less than the network size ($d < d_t$). To minimize the interaction between the diffusing nanorod and matrix, the nanorod surface is grafted with phenyl groups that are chemically similar to the polystyrene matrix chains. Our results show that the nanorod diffusion is as much as 1000× faster than that predicted by the continuum Stokes−Einstein prediction using the measured bulk viscosity of the matrix. This enhancement in nanorod diffusion is attributed to a reduced local friction that results from the decoupling of nanorod motion (i.e., parallel direction) and polymer dynamics described by the relaxation of matrix chains by reptation.

TiO_2 NRs (L = 43.1 nm and d = 4.6 nm) were synthesized using standard Schlenk-line techniques, in the presence of oleic acid and oleylamine and using $TiCl_4$ as precursor. Ligands were subsequently displaced by treatment with $NOBF_4$ to allow further functionalization. Details can be found elsewhere.[22] Further, NR surface modification using (chloromethyl)-dimethyl phenylsilane facilitates the dispersion of NRs in PS (M = 9, 65, 160, 650, and 2000 kDa), as shown in Figure 2. A

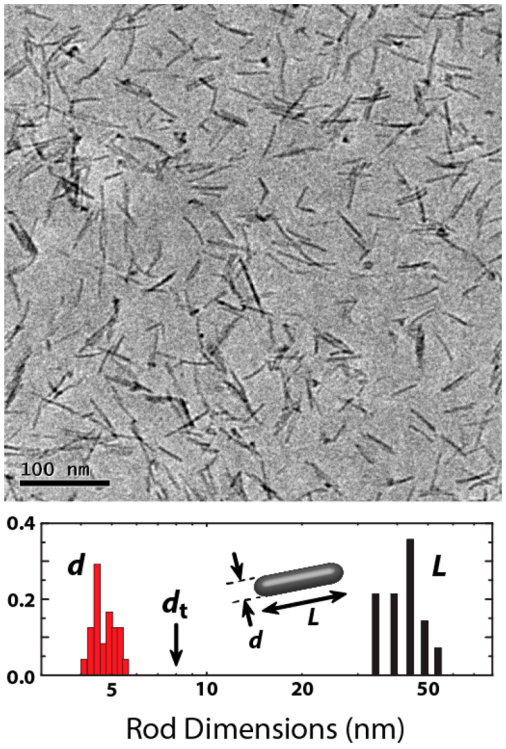

Figure 2. Transmission electron micrograph depicting the dispersion of phenyl-capped TiO_2 NRs in a PS matrix (M = 650 kDa, ϕ_{NR} = 0.01). Histogram shows the diameter (d) and length (L) distributions, where d_t denotes the tube diameter of PS (~8 nm).

mixture of methyl ethyl ketone and dimethylformamide was used as a solvent. Bilayers were prepared with a thin (~300 nm) PS (M = 9−2000 kDa) film containing TiO_2 NRs (ϕ_{NR} = 0.01) over a thick (~10 μm) PS matrix with the same M and annealed in a vacuum oven at T = 190 °C from minutes to days (see Supporting Information for NR dispersion after thermal annealing). The dilution of the NRs in the tracer film was required to ensure unhindered NR diffusion into the matrix. Tracer diffusion coefficients were determined by fitting the TiO_2 volume fraction profiles determined by Rutherford Backscattering Spectrometry (RBS). Using appropriate boundary and initial conditions, $\phi_{TiO_2}(x)$ is given by

$$\phi_{TiO_2}(x) = \frac{1}{2}\left[\mathrm{erf}\left(\frac{l-x}{\sqrt{4Dt}}\right) + \mathrm{erf}\left(\frac{l+x}{\sqrt{4Dt}}\right)\right] \quad (4)$$

DOI: 10.1021/acsmacrolett.5b00348
ACS Macro Lett. 2015, 4, 952−956

where erf, t, and l are the error function, annealing time, and initial tracer thickness, respectively. This equation is convoluted with the instrumental depth resolution, a Gaussian function, and chi squared fitting is used to determine the best fit of eq 4 to the experimental profile.

For rheology measurements, the linear viscoelastic behavior of the nanocomposites was measured on a Rheometrics Solids Analyzer II using a sandwich fixture. Samples were annealed at 200 °C for 20 min before testing. The modulus was measured using a frequency sweep under a N_2 atmosphere at 170, 190, 210, and 230 °C with 0.5% strain. These were combined using time−temperature superposition to yield a master curve, and then, zero shear viscosity was obtained according to the literature at 190 °C.[23]

The local polymer dynamics of PS and PS/NR was measured by rheology. Akcora et al.[24] reported solid-like mechanical reinforcement in polymer nanocomposites due to nonuniform dispersion (i.e., interconnected NPs) of spherical NPs at loadings greater than 5 wt %. For the PS(M)/NR blends in this paper, in the low frequency region, the storage and loss moduli did not exhibit plateaus, consistent with a uniform NR dispersion at each M. Moreover, the lack of a plateau indicates that the NRs did not induce solid-like behavior by percolation or clustering, which is only expected above $\phi_c \sim 0.04$, the 3D percolation threshold for NRs with an aspect ratio of 9.[25] For $\phi_{NR} \sim 0.01$, Figure 3 shows that the zero-shear viscosities of

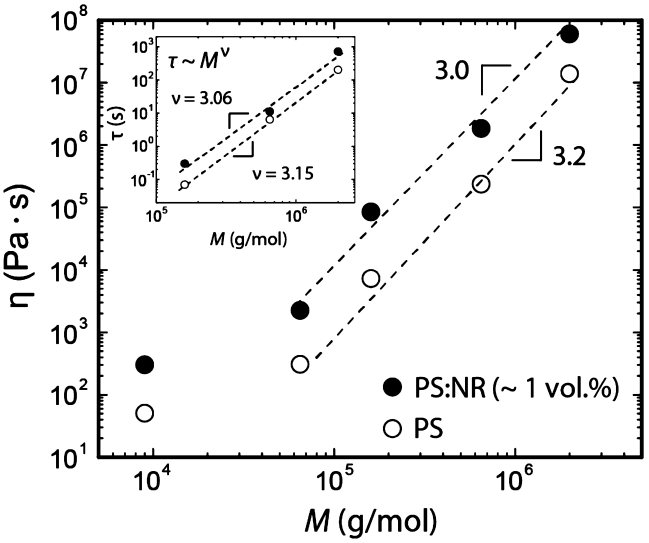

Figure 3. Zero-shear viscosity of pure PS and PS/NR blends ($\phi_{NR} = \sim 0.01$) at T = 190 °C as a function of molecular weight (M = 9−2000 kDa). For M = 9k (unentangled), η was obtained by extrapolation assuming Rouse dynamics, $\eta \sim M^1$. The dashed lines show the viscosity scaling for PS and PS/NR above the entanglement molecular weight are similar, namely, $M^{3.0}$ and $M^{3.2}$, respectively. The inset shows the molecular weight dependence of the relaxation time ($\tau \sim M^{\nu}$) determined from the crossover frequency of the storage and loss moduli.

blends are a factor of ∼5 greater than pure PS at each M. Although $d < d_t$, the increase in viscosity in Figure 3 is expected because NR length is significantly greater than d_t (c.f., Figure 2). Similarly, the viscosity of polymer blends with thin ($<d_t$) clay particles increases with clay concentration, consistent with predictions by Einstein.[26]

NR diffusion was measured as a function of matrix molecular weight. For an annealed bilayer, Figure 4a shows a

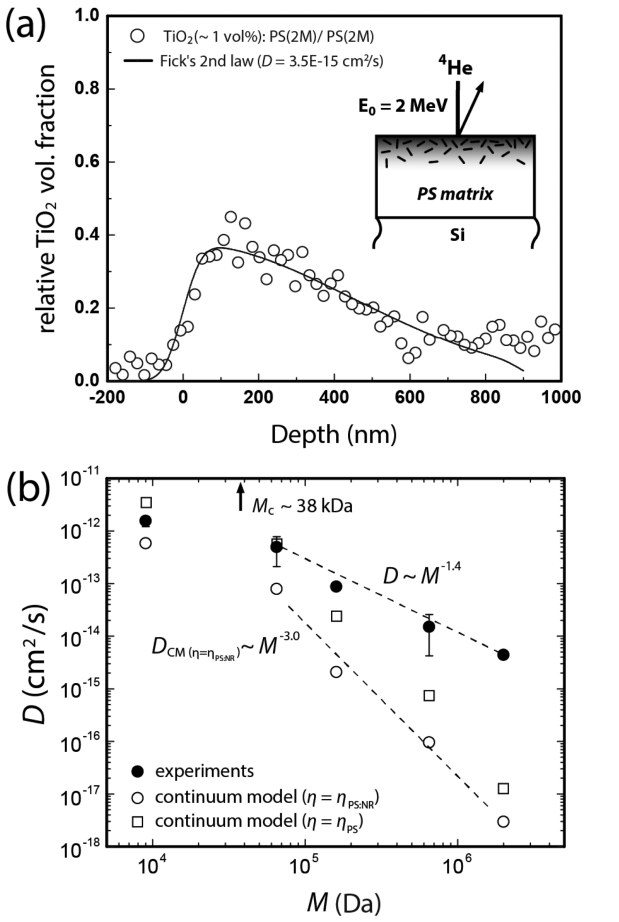

Figure 4. (a) Depth profile of TiO_2 in a PS matrix (M = 2000 kDa) after annealing at 190 °C for 24 h. (b) Theoretical (open circles and squares) and measured (closed circles) diffusion coefficients of NRs in PS matrices (M = 9−2000 kDa) at 190 °C. The critical molecular weight for PS entanglement, M_e, is 38 kDa.[27] The error bars represent the standard deviation from multiple samples, which is smaller than the symbol size for M = 9, 160, and 2000 kDa. The error due to ligand size is also smaller than the symbol size.

representative NR volume fraction profile in a highly entangled PS matrix (M = 2000 kDa), where the solid line eq 4 represents a best fit to the experimental data (circles) using $D = 3.5 \times 10^{-15}$ cm^2 s^{-1}. For comparison with the measured diffusion coefficients, theoretical values based on the Einstein relation eqs 1−3 were calculated using the viscosity shown in Figure 3 for pure PS (open squares) and PS/NR ($\phi_{TiO2} = 0.01$) blends (open circles). The PS/NR (1 vol %) viscosity was chosen to represent the bulk viscosity that NRs may experience in the concentration gradient shown in Figure 4a. Note that the scaling behavior in Figure 4b is independent of whether the PS or PS/NR bulk viscosity is used.

Figure 4b shows the experimental and continuum predictions for NR diffusion coefficients in polystyrene matrices ranging from unentangled to entangled and provides insights into the correlations between NR and the polymer dynamics. Because $D_{CM} \sim \eta^{-1}$ in the continuum model, the M dependence of the measured bulk viscosity (i.e., $\eta \sim M^{3.0}$) is responsible for the $D_{CM} \sim M^{-3.0}$ scaling in Figure 4b (lower dashed line). This behavior reflects the strong coupling between NR diffusion and

DOI: 10.1021/acsmacrolett.5b00348
ACS Macro Lett. 2015, 4, 952−956

chain relaxation inherent in the continuum model. Thus, NR diffusion slows down dramatically as M increases for $M > M_c$. However, the measured D values (closed circles) are greater than those predicted by the continuum model. Furthermore, the difference between D (measured) and D_{CM} (predicted) increases from about 1 to 3 orders of magnitude as M increases from 65 to 2000 kDa, because D only weakly scales with M, $D \sim M^{-1.4}$ (upper dashed line). This weak M dependence for D, relative to $D_{CM} \sim M^{-3.0}$, implies that the dynamics of NR diffusion is partially decoupled from the entangled matrix polymers that relax by reptation. For comparison, complete decoupling would lead to diffusion that is independent of molecular weight.

This enhanced diffusion of NRs is in good agreement with the diffusion of small NPs predicted by Brochard-Wyart and de Gennes.[13] For spherical NPs to diffuse through an entanglement mesh, the relaxation of an entire chain is required when particle size is much larger than d_t. When the NP size becomes smaller than the entanglement mesh size, the local relaxation of chain segments is sufficient to accommodate the diffusive motion of NPs. In the limit of small NPs (i.e., monomer size), NP diffusion becomes independent of matrix molecular weight as NPs freely move within the entangled network. On the other hand, nanorod diffusion is highly anisotropic when $D_{\parallel}$ is greater than $D_{\perp}$. For NRs to move perpendicularly (Figure 1b), the entire chain must relax, as required for large spherical NPs; however, NRs moving parallel to their length only experience a local nanoviscosity because $d < d_t$. Thus, Brochard-Wyart and de Gennes predict that the net NR diffusion is faster than that predicted by D_{CM} using the bulk viscosity in Figure 4b. When L is sufficiently long (i.e., $L > d^2/4a$), lateral friction dominates the parallel diffusion of NRs,[13] so that for NRs to continue to diffuse in the parallel direction adjacent openings in the entanglement mesh must (partially) align (c.f., Figure 1). Thus, a complete description of NR diffusion should also account for the rotation of NRs as they diffuse through the entanglement mesh.

The rotational motion of NRs is inversely proportional to bulk viscosity and decreases strongly as L increases as $D_{rotational} \sim L^{-3}$. Here L = 43 nm, about 5× larger than d_t, so that NRs thread about five entanglement meshes. Although rotational motion is constrained by entanglements, NRs can locally rotate by the segmental mobility of matrix subchains. For comparison, entangled matrix chains (160−2000 kDa) are expected to exhibit high segmental mobility because chain diffusivity is about an order of magnitude greater than NR diffusivity at the same temperature (i.e., T = 190 °C). Therefore, we propose that segmental relaxation of matrix chains near the NR allows for rotation-mediated translational motion of NRs, which may explain the $M^{-1.4}$ scaling suggestive of the weak coupling in Figure 4b (closed circles).

Figure 5 shows the experimental diffusion coefficients normalized by the continuum prediction using either PS or PS/NR viscosities. For M = 9k (unentangled), the measured diffusion coefficient is in good agreement with the continuum theory, possibly because the NR diameter and length are both larger than $2R_g$. However, in both cases, the normalized D increases strongly as the average number of entanglements, M/M_e, increases. Previously, deviations from SE diffusion in melts were observed for spherical NPs having diameters comparable to the entanglement mesh size ($d/d_t \sim 1-2$).[10] Using GLE theory and MD simulations, Kalathi et al. reported that the matrix molecular weight dependence of NP diffusion depends on NP size due to spontaneous fluctuations in the entanglement mesh.[14] In a similar way, for high molecular weight polymer melts, the constraint release of subchains adjacent to the NRs allow the entanglement mesh to align and NRs to rotate and thereby to facilitate parallel diffusion. For high M, these results indicate that nanoscale fillers (e.g., isotropic NPs or anisotropic NRs) with dimensions smaller than the entanglement mesh interact with a discrete medium rather than a continuous medium, where macroscopic viscosity dictates diffusion. Therefore, the increase in the normalized diffusion coefficients as M/M_e increases (Figure 5) may be attributed to the partial decoupling of NR motion and polymer dynamics.

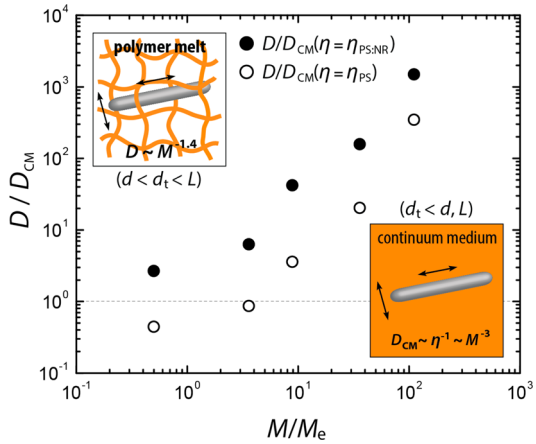

Figure 5. NR diffusion coefficients (D) normalized by the diffusion coefficients predicted by the continuum model (D_{CM}) as a function of the average number of entanglements per PS matrix chain. Upper and lower insets show NRs in an entangled polymer melt ($d < d_t < L$) and continuum medium ($d_t < d, L$), where diffusion scales as $M^{-1.4}$ and $M^{-3.0}$, respectively.

In conclusion, the diffusion of nanorods with a diameter smaller than the entanglement mesh size or tube diameter (i.e., $d < d_t$) of the polymer matrix is observed to be up to 3 orders of magnitude faster than the continuum model that assumes a uniform hydrodynamic medium. This enhanced diffusion likely results from decoupling of nanorod diffusion from the relaxation of matrix chains that surround the nanorod due the relative size of the NR diameter to the matrix network, $d < d_t$. Because NRs can rotate and tilt within the confining network to enter an adjacent entanglement mesh, NR motion is not completely decoupled from polymer dynamics, because the NR is confined within about five networks. Therefore, the weak M dependence of D ($\sim M^{-1.4}$) implies that the local viscosity of chain segments along the NR length ($\eta \sim \eta_m L a^{-1}$) influences dynamics at the NR/polymer interface. However, a comprehensive understanding of the mechanism for NR diffusion incorporating both rotational and translational motion is still unclear. Theoretical studies similar to Kalathi et al.[14] should be extended to nanorods to clarify the relationship between the diffusion of anisotropic particles in an entangled polymer melt and the fundamental parameters such as matrix molecular weight, entanglement mesh size, and particle dimensions.

■ ASSOCIATED CONTENT

Supporting Information

Transmission electron micrograph depicting the stable dispersion of TiO_2 NRs in PS matrix. The Supporting

DOI: 10.1021/acsmacrolett.5b00348
ACS Macro Lett. 2015, 4, 952−956

Information is available free of charge on the ACS Publications website at DOI: 10.1021/acsmacrolett.5b00348.

(PDF)

AUTHOR INFORMATION

Corresponding Author

*E-mail: composto@seas.upenn.edu.

Notes

The authors declare no competing financial interest.

ACKNOWLEDGMENTS

This research was primarily supported by the National Science Foundation NSF/EPSRC Materials World Network DMR-1210379 (R.J.C., K.I.W.) and through the Nano/Bio Interface Center at the University of Pennsylvania, Grant DMR08-32802 (M.C.), the EPSRC EP/5065373/1 (N.C.), and Dupont Central Research and Development (R.J.C.). Support was also provided by the NSF/MRSEC-DMR 11-20901 (K.I.W., R.J.C.) and Polymer Programs DMR09-07493 (R.J.C.). This study was financially supported by research fund of Chungnam National University (J.C.). This work is supported by the National Research Foundation of Korea (NRF) grant funded by the Korean government (MSIP: Ministry of Science, ICT and Future Planning; No. NRF-2015M2B2A4033360). C.B.M. is grateful for the support of the Richard Perry University Professorship. Kenneth S. Schweizer (UIUC) and Michael Rubinstein (UNC) are gratefully acknowledged.

REFERENCES

(1) Winey, K. I.; Vaia, R. A. *MRS Bull.* **2007**, *32*, 314−319.
(2) Lin, M. Y.; Lindsay, H. M.; Weitz, D. A.; Ball, R. C.; Klein, R.; Meakin, P. *Nature* **1989**, *339*, 360−362.
(3) Mackay, M. E.; Tuteja, A.; Duxbury, P. M.; Hawker, C. J.; Horn, B. V.; Guan, Z.; Chen, G.; Krishnan, R. S. *Science* **2006**, *311*, 1740−1743.
(4) Bockstaller, M. R.; Mickiewicz, R. A.; Thomas, E. L. *Adv. Mater.* **2005**, *17*, 1331−1349.
(5) Lopes, W. A.; Jaeger, H. M. *Nature* **2001**, *414*, 735−738.
(6) Huynh, W. U.; Dittmer, J. J.; Alivisatos, A. P. *Science* **2002**, *295*, 2425−2427.
(7) Talapin, D. V.; Murray, C. B. *Science* **2005**, *310*, 86−89.
(8) Yamamoto, U.; Schweizer, K. S. *J. Chem. Phys.* **2011**, *135*, 224902.
(9) Yamamoto, U.; Schweizer, K. S. *Macromolecules* **2015**, *48*, 152.
(10) Tuteja, A.; Mackay, M. E.; Narayanan, S.; Asokan, S.; Wong, M. S. *Nano Lett.* **2007**, *7*, 1276−1281.
(11) Grabowski, C. A.; Mukhopadhyay, A. *Macromolecules* **2014**, *47*, 7238−7242.
(12) Omari, R. A.; Aneese, A. M.; Grabowski, C. A.; Mukhopadhyay, A. *J. Phys. Chem. B* **2009**, *113*, 8449−8452.
(13) Wyart, F. B.; de Gennes, P. G. *Eur. Phys. J. E: Soft Matter Biol. Phys.* **2000**, *1*, 93−97.
(14) Kalathi, J. T.; Yamamoto, U.; Schweizer, K. S.; Grest, G. S.; Kumar, S. K. *Phys. Rev. Lett.* **2014**, *112*, 108301.
(15) Bronstein, N. D.; Li, L.; Xu, L.; Yao, Y.; Ferry, V. E.; Alivisatos, A. P.; Nuzzo, R. G. *ACS Nano* **2014**, *8*, 44−53.
(16) Chhetri, R. K.; Blackmon, R. L.; Wu, W.- C.; Hill, D. B.; Button, B.; Casbas-Hernandez, P.; Troester, M. A.; Tracy, J. B.; Oldenburg, A. L. *Proc. Natl. Acad. Sci. U. S. A.* **2014**, *111*, E4289−E4297.
(17) Riseman, J.; Kirkwood, J. G. *J. Chem. Phys.* **1950**, *18*, 512−516.
(18) Eimer, W.; Pecora, R. *J. Chem. Phys.* **1991**, *94*, 2324−2329.
(19) Haghighi, M.; Tahir, M. N.; Tremel, W.; Butt, H.-J.; Steffen, W. *J. Chem. Phys.* **2013**, *139*, 064710.
(20) Tsay, J. M.; Doose, S.; Weiss, S. *J. Am. Chem. Soc.* **2006**, *128*, 1639−1647.
(21) Alam, S.; Mukhopadhyay, A. *Macromolecules* **2014**, *47*, 6919−6924.
(22) Gordon, T. R.; Cargnello, M.; Paik, T.; Mangolini, F.; Weber, R. T.; Fornasiero, P.; Murray, C. B. *J. Am. Chem. Soc.* **2012**, *134*, 6751−6761.
(23) Rubinstein, M.; Colby, R. H. *Polymer Physics*; Oxford University Press: New York, 2003.
(24) Akcora, P.; Liu, H.; Kumar, S. K.; Moll, J.; Li, Y.; Benicewicz, B. C.; Schadler, L. S.; Acehan, D.; Panagiotopoulos, A. Z.; Pryamitsyn, V.; Ganesan, V.; Ilavsky, J.; Thiyagarajan, P.; Colby, R. H.; Douglas, J. F. *Nat. Mater.* **2009**, *8*, 354−359.
(25) Mutiso, R. M.; Sherrott, M. C.; Li, J.; Winey, K. I. *Phys. Rev. B: Condens. Matter Mater. Phys.* **2012**, *86*, 214306.
(26) Einstein, A. *Ann. Phys.* **1906**, *324*, 371.
(27) Kramer, E. J. Microscopic and Molecular Fundamentals of Crazing. *Crazing in Polymers: Advances in Polymer Science*; Springer: Berlin; Heidelberg, 1983; Vol. *52*−*3*, p 1.

DOI: 10.1021/acsmacrolett.5b00348
ACS Macro Lett. 2015, 4, 952−956